

This is the accepted manuscript made available via CHORUS. The article has been published as:

## Shape coexistence along $N=40$

S. N. Liddick *et al.*

Phys. Rev. C **84**, 061305 — Published 27 December 2011

DOI: [10.1103/PhysRevC.84.061305](https://doi.org/10.1103/PhysRevC.84.061305)

# Shape coexistence along $N = 40$

S. N. Liddick,<sup>1,2</sup> S. Suchyta,<sup>1,2</sup> B. Abromeit,<sup>1</sup> A. Ayres,<sup>3</sup> A. Bey,<sup>3</sup> C. R. Bingham,<sup>3</sup> M. Bolla,<sup>1</sup> M. P. Carpenter,<sup>4</sup> L. Cartegni,<sup>3</sup> C. J. Chiara,<sup>4,5</sup> H. L. Crawford,<sup>6</sup> I. G. Darby,<sup>7</sup> R. Grzywacz,<sup>3</sup> G. Gürdal,<sup>8</sup> S. Ilyushkin,<sup>9</sup> N. Larson,<sup>1,2</sup> M. Madurga,<sup>3</sup> E. A. McCutchan,<sup>4</sup> D. Miller,<sup>3</sup> S. Padgett,<sup>3</sup> S. V. Paulauskas,<sup>3</sup> J. Pereira,<sup>1</sup> M. M. Rajabali,<sup>7</sup> K. Rykaczewski,<sup>10</sup> S. Vinnikova,<sup>1,2</sup> W. B. Walters,<sup>5</sup> and S. Zhu<sup>4</sup>

<sup>1</sup>*National Superconducting Cyclotron Laboratory, Michigan State University, East Lansing, MI 48824, USA*

<sup>2</sup>*Department of Chemistry, Michigan State University, East Lansing, MI 48824, USA*

<sup>3</sup>*Department of Physics and Astronomy, University of Tennessee, Knoxville, TN 37996, USA*

<sup>4</sup>*Physics Division, Argonne National Laboratory, Argonne, IL 60439, USA*

<sup>5</sup>*Department of Chemistry and Biochemistry, University of Maryland, College Park, MD 20742, USA*

<sup>6</sup>*Nuclear Science Division, Lawrence Berkeley National Laboratory, Berkeley, CA 94720, USA*

<sup>7</sup>*Instituut voor Kern- en Stralingsfysica, Katholieke Universiteit Leuven, B-3001 Leuven, Belgium*

<sup>8</sup>*Nuclear Engineering Division, Argonne National Laboratory, Argonne, IL 60439, USA*

<sup>9</sup>*Department of Physics and Astronomy, Mississippi State University, MS 39762, USA*

<sup>10</sup>*Physics Division, Oak Ridge National Laboratory, Oak Ridge, TN 37831, USA*

The low-energy level structures of  $^{64}\text{Mn}_{39}$  and  $^{66}\text{Mn}_{41}$  were investigated through both the decay of Mn metastable states and the population of levels following the  $\beta$  decay of  $^{64}\text{Cr}$  and  $^{66}\text{Cr}$ . The deduced level schemes and tentatively assigned spins and parities suggest the coexistence of spherical and deformed configurations above and below  $N = 40$  for the odd-odd Mn isotopes. The low-energy deformed configurations are attributed to the coupling between a proton in a  $K = 1/2^-$  level with neutrons in either the  $K = 1/2^-$  or  $K = 3/2^+$  levels originating from the  $\pi p_{3/2}$ ,  $\nu p_{1/2}$ , and  $\nu g_{9/2}$  single-particle states, respectively.

PACS numbers: 23.35.+g 23.40.-s 27.50.+e

The nucleus is a complex many-body system and can be described by a mix of single-particle and collective excitation modes. The relative importance of the two excitations is predominantly dictated by the distribution of single-particle states near the Fermi surface for a given nucleus. A major development in understanding the structure of the nucleus was the realization that the single-particle level density at a particular proton and neutron number is not a smooth function of energy, but fluctuates, giving rise to energy gaps between clusters of single-particle states [1]. Near stable nuclei, the energy gaps occur at characteristic values of neutron and proton number: 2, 8, 20, 28, 50, 82 and, for neutrons, 126. Nuclei with these numbers of protons or neutrons are more stable than their neighboring isotopes, have low-energy level structures dominated by single-particle excitations, and are spherical in shape.

The inherent stability of nuclei at these proton and neutron values is akin to the chemical inertness of the noble gases due to the filling of atomic orbitals. However, unlike the atomic case, the nuclear single-particle level ordering is not constant across all nuclei. Various effects can lead to the rearrangement of single-particle states [2, 3], influencing the magnitude of the energy gaps and, in some cases, eliminating them completely [4]. As the magnitude of the single-particle energy gap is reduced it becomes easier to excite nucleons across a shell gap, leading to particle-hole intruder configurations [5]. While the excitation energy of such a state is expected to be on the order of the size of the energy gap, possible proton-neutron interactions can lead to significant gains in binding energy, stabilizing the system and

reducing the overall energy required for such excitations. If the intruder states have a significantly different deformation as compared to the ground state, two competing nuclear shapes can coexist at similar energies leading to the possibility of shape isomerism.

A neutron shell gap at  $N = 40$  was proposed based on spectroscopic data from  $^{68}\text{Ni}$  [6, 7] and attributed to a large energy separation between the neutron pf shell states and the  $g_{9/2}$  single-particle state. Accumulated experimental data on nuclei in the vicinity of  $^{68}\text{Ni}$  has since shown the  $N = 40$  gap to be quite fragile [8–10]. Furthermore, evidence for the increasing influence of the intruder neutron  $g_{9/2}$  single-particle state and the development of deformation has accumulated in the Fe and Mn isotopes [11–14]. Large-scale shell-model calculations along  $N = 40$  near  $^{68}\text{Ni}$  have had success interpreting even-even nuclei in this region and suggest a sharp transition from spherical to prolate deformed nuclei with the removal of two protons from  $^{68}\text{Ni}$  to  $^{66}\text{Fe}$  [15]. The change is attributed to the migration of the neutron  $f_{5/2}$  single-particle state, which increases in energy as protons are removed from the  $f_{7/2}$  single-particle state in a progression from Ni to Ca and eventually crosses through the  $N = 40$  energy gap near the Mn isotopic chain. However, the model has yet to be applied to odd-odd nuclei along  $N = 40$ , and other experimental findings in odd-A nuclei have suggested the influence of shape coexistence must be considered as well [16, 17].

This Letter reports on the low-energy structure of  $^{64}\text{Mn}_{39}$  and  $^{66}\text{Mn}_{41}$  populated through two separate mechanisms,  $\beta$ -decay and projectile fragmentation techniques. The first identification of excited spherical iso-

meric states coexisting with a deformed ground states in odd-odd Mn nuclei straddling  $N = 40$ , combined with prior results, experimentally demonstrate an extensive region of shape coexistence around  $N = 40$ .

The neutron-rich nuclei of interest were produced at the National Superconducting Cyclotron Laboratory (NSCL) in two different experiments by impinging either a 140-MeV/A  $^{76}\text{Ge}$  beam or a 130-MeV/A  $^{86}\text{Kr}$  beam onto a  $^9\text{Be}$  target located at the object position of the A1900 fragment separator [18]. The resulting fragmentation products were separated using the A1900 and a thin ( $\sim 20\text{-mg/cm}^2$ ) Kapton wedge located at the intermediate dispersive image. The full momentum acceptance of the device ( $\sim 5\%$ ) was used for both experiments. The fragmentation of the  $^{86}\text{Kr}$  primary beam was used to investigate the beta-decay of  $^{64,66}\text{Cr}$  into states of  $^{64,66}\text{Mn}$  while the  $^{76}\text{Ge}$  primary beam was used to populate  $^{64,66}\text{Mn}$  isomeric states.

The cocktail beams were characterized event-by-event using energy-loss and time-of-flight techniques, and delivered to the Beta Counting Station (BCS) [19]. The  $\beta$  decays were correlated with implanted ions in analysis based on both position and temporal information. Isomeric and  $\beta$ -delayed  $\gamma$  rays were detected using 16 Ge detectors from SeGA [20]. The total efficiency of the array was measured to be 8.7% at the 662-keV  $^{137}\text{Cs}$  transition. All detector data were read out using the NSCL Digital Data Acquisition System (DDAS) whose hardware is described in Ref. [21]. Individual channels were independently triggered, time stamped, written to disk, and those channels triggering within a  $10\text{ }\mu\text{s}$  time window were grouped into events in software. The overall implantation rate was kept low ( $< 50\text{ Hz}$ ). The SeGA detectors were ungated due to the low dead time of the DDAS allowing for the exploration of long-lived ( $T_{1/2} \sim$  milliseconds) isomeric states. Isomeric  $\gamma$ -ray transitions were correlated in software with the last implanted ion and were distinguished from background on the basis of their decay curves, constructed from the time difference between the  $\gamma$  ray and the previously implanted ion, and  $\gamma$ - $\gamma$  coincidences.

Low-energy states in  $^{64}\text{Mn}$  and  $^{66}\text{Mn}$  were populated through both the  $\beta$  decay of  $^{64}\text{Cr}$  and  $^{66}\text{Cr}$  and the decay of the metastable states  $^{64m}\text{Mn}$  and  $^{66m}\text{Mn}$ . The  $\beta$ -delayed  $\gamma$ -ray spectrum observed within 500 ms following the implantation of a  $^{64}\text{Cr}$  ion is shown in Fig. 1(a). The experimental decay curve was fit with contributions from  $^{64}\text{Cr}$ ,  $^{64}\text{Mn}$ , and a constant background. The  $^{64}\text{Mn}$  half-life was fixed in the fit at a value of 90 ms [8, 22] and the extracted  $^{64}\text{Cr}$  half-life was 44(3) ms, in agreement with previous measurements [23]. Two  $\gamma$  rays can be assigned to  $^{64}\text{Mn}$  following the  $\beta$  decay of  $^{64}\text{Cr}$ : the 186-keV  $\gamma$  ray previously observed in Ref. [23], and a new transition at 962 keV that defines a state at 1149 keV, see Fig. 3. The coincidence spectrum obtained by gating on the 962-keV transition is shown as an inset in Fig. 1(a). From the observed  $\gamma$ -ray intensity, the absolute efficiency of SeGA, the  $\beta$ -detection efficiency, and

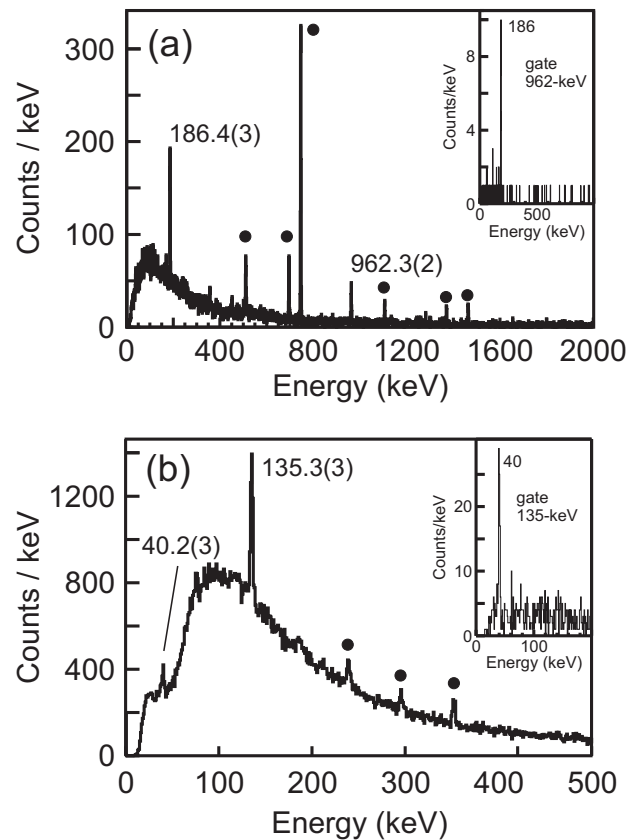


FIG. 1. (a)  $\beta$ -delayed  $\gamma$  rays within 500 ms following the implantation of a  $^{64}\text{Cr}$  ion. Transitions assigned to the decay of  $^{64}\text{Cr}$  are labeled with their energies in keV. Gamma rays from daughter and granddaughter activities are marked by full circles. (inset)  $\gamma$ - $\gamma$  coincidence spectrum obtained by gating on the 962-keV transition. (b) Isomeric  $\gamma$  rays detected within 5 ms following the implantation of a  $^{64m}\text{Mn}$  ion. Transitions assigned to the decay of  $^{64m}\text{Mn}$  are labeled with their energies in keV. Natural background transitions are marked by full circles. (inset)  $\gamma$ - $\gamma$  coincidence spectrum obtained by gating on the 135-keV transition.

the number of ions detected, the  $\beta$ -decay feeding to the ground, 186-keV, and 1149-keV states could be extracted and are 92(2)%,  $< 3\%$ , and 8(2)%, respectively. The  $\beta$  decay of the  $0^+$   $^{64}\text{Cr}$  ground state proceeds predominantly through a direct transition to the  $^{64}\text{Mn}$  ground state, suggesting a ground-state spin and parity of  $1^+$  for  $^{64}\text{Mn}$ . The remaining  $\beta$ -decay intensity goes to an excited state at 1149 keV which is also tentatively assigned as a  $1^+$  state. Contrary to Ref. [23], there is no appreciable feeding to the intermediate state at 186 keV and it is tentatively assigned a  $2^+$  spin and parity.

The  $\gamma$  rays detected within 5 milliseconds following an implanted  $^{64m}\text{Mn}$  ion are shown in Fig. 1(b). Since the only requirement in Fig. 1(b) was that a  $\gamma$  ray was detected within a few milliseconds following the implanted ion, natural background radiation is observable in the spectrum, as marked. The isomeric transitions at 40 and 135 keV are clearly observable above the natural back-

ground and have the same  $\gamma$ -gated half-life, within error, of  $400(40) \mu\text{s}$ , which agrees with the previously obtained lower limit [24]. The two transitions are in coincidence with each other (see inset of Fig. 1(b)) leading to the observed  $^{64}\text{Mn}$  low-energy structure presented in Fig. 3. The isomeric state in  $^{64}\text{Mn}$  was previously suggested to decay by an  $M2$  transition [24]. The half-life of the 175-keV state in  $^{64}\text{Mn}$  is consistent with an  $M2$  multipolarity for the 135-keV transition based on Weisskopf estimates. The hindrance,  $F$ , of the 135-keV transition with respect to the Weisskopf estimate is  $F = (T_{1/2, \text{exper}}/T_{1/2, \text{Weisskopf}}) = 9$ . Assuming the level scheme presented in Fig. 3, and correcting for the  $\gamma$ -ray detection efficiency, the intensity of the 40-keV transition is lower than expected as compared to the 135-keV transition. The missing intensity in the 40-keV transition in  $^{64}\text{Mn}$  suggests an  $E1$  multipolarity based on the inferred electron conversion of  $1.6(7)$ , slightly higher than the value of  $0.6$  expected for an  $E1$  transition but in agreement with a previously reported value [25]. Starting from the  $1^+$  ground-state spin and parity assigned through  $\beta$  decay, an  $M2$ - $E1$  isomeric cascade tentatively suggests spins and parities of  $2^-$  and  $4^+$  to the 40-keV and 175-keV levels, respectively.

The  $\beta$ -delayed  $\gamma$ -ray spectrum observed within 100 ms following the implantation of a  $^{66}\text{Cr}$  ion is shown in Fig. 2(a). The half-life of  $^{66}\text{Cr}$  was determined to be  $24(2)$  ms based on a fit to the experimental decay curve which included contributions from the decay of  $^{66}\text{Cr}$ ,  $^{66}\text{Mn}$ , and a constant background. The half-life of  $^{66}\text{Mn}$  was fixed in the fit at a value of 65 ms [8, 22]. The  $^{66}\text{Cr}$  half-life is slightly higher than previously reported [22, 23] which is likely due to the increased statistics.

Only one  $\gamma$  ray at 653 keV was observed following the  $\beta$  decay of  $^{66}\text{Cr}$ . Similar to  $^{64}\text{Mn}$ , a large percentage of the  $\beta$ -decay feeding,  $67(12)\%$ , proceeds to the ground state of  $^{66}\text{Mn}$  with only  $33(12)\%$  populating the excited state. The observation of such a large ground-state feeding suggests a spin and parity of  $1^+$  for the  $^{66}\text{Mn}$  ground state, although it should be noted that the ground-state  $\beta$ -decay feeding is an upper limit and low-intensity  $\gamma$ -ray transitions directly to the ground state may not have been observed. The  $\gamma$  rays detected within 7 milliseconds following the implantation of a  $^{66m}\text{Mn}$  ion ( $T_{1/2}=780(40) \mu\text{s}$ ) are shown in Fig. 2(b). Three isomeric transitions were observed in the spectrum at 170, 295, and 251 keV with identical half-lives within errors. The 295-keV transition was observed in coincidence with the 170-keV transition. An additional transition at 44 keV was observed in coincidence with the 251-keV transition, see Fig. 2b. The 44-keV transition is assigned an  $E1$  multipolarity based on the deduced electron conversion coefficient from the 251-44-keV  $\gamma$ -ray cascade of  $1.4(8)$ , analogous to the 40-keV transition in  $^{64m}\text{Mn}$ .

The 170-keV transition is assigned as an  $M2$  transition based on Weisskopf estimates with a hindrance of  $F = 60$ . The 295-keV and 251-keV transitions are limited to multipolarities of  $\lambda \leq 2$  and the 44-keV transition to

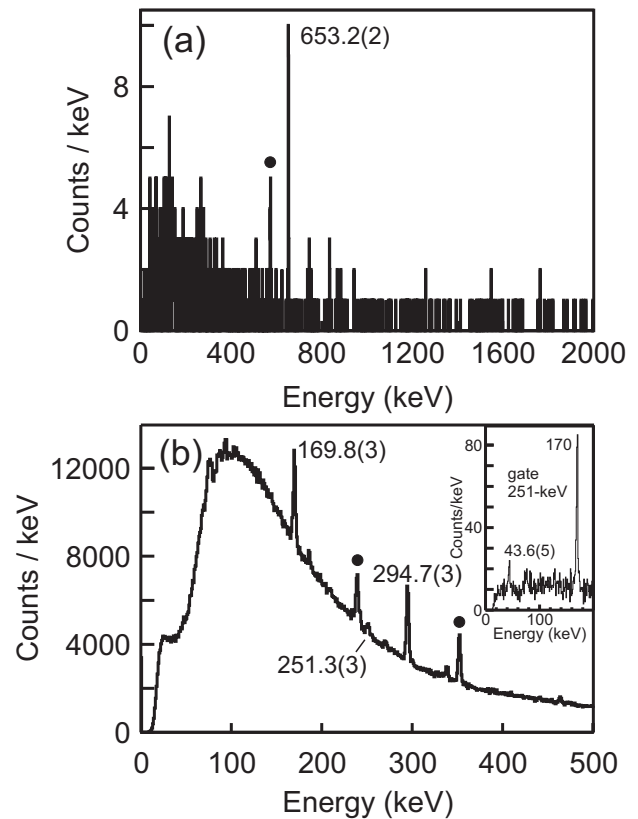


FIG. 2. (a)  $\beta$ -delayed  $\gamma$  rays following the implantation of a  $^{66}\text{Cr}$  ion within 100 ms. Transitions assigned to the decay of  $^{66}\text{Cr}$  are labeled with their energies in keV. A  $\gamma$  ray from the daughter activity is marked by a full circle. (b) Isomeric  $\gamma$  rays following the decay of  $^{66m}\text{Mn}$ . Transitions assigned to the decay of  $^{66m}\text{Mn}$  are labeled with their energies in keV. Natural background transitions are marked by circles. (inset)  $\gamma$ - $\gamma$  coincidence spectrum obtained by gating on the 251-keV transition.

$\lambda \leq 1$  due to the lack of observable half-lives from the respective excited states.

The low-energy level schemes for  $^{64,66}\text{Mn}$  are shown in Fig. 3 with tentatively proposed spin and parity assignments. For the levels fed by  $\beta$  decay,  $\beta$ -decay branching ratios and  $\log ft$  values are shown to the left of the state. The microscopic structure of  $^{64}\text{Mn}$  and  $^{66}\text{Mn}$  can be understood by referring to single proton and neutron occupancies inferred from neighboring nuclei. The configuration of the odd proton in  $^{64,66}\text{Mn}$  can be inferred from the  $^{67}\text{Co}$  isotopes. In  $^{67}\text{Co}$ , just one proton removed from  $^{68}\text{Ni}$ , the ground state of  $^{67}\text{Co}$  was attributed to the spherical  $\pi f_{7/2}^{-1}$  configuration. An unexpected  $1/2^-$  isomeric state in  $^{67}\text{Co}$  was explained by the presence of a prolate-deformed shape isomer only a few hundred keV above the spherical ground state [17]. An inspection of the proton Nilsson orbits from Ref. [26] indicates a steeply down-sloping  $K = 1/2^-$  level originating from the spherical proton  $p_{3/2}$  single-particle state which drops below the  $K = 7/2^-$  level of the  $f_{7/2}$  single-particle state

at a deformation,  $\beta$ , of  $\sim 0.2$ . The presence of a deformed proton state in  $^{67}\text{Co}$  and the consistent drop in the energy of the  $1/2^-$  levels in the odd-A Co isotopes starting at  $N = 36$  [17] indicates that the deformed proton configuration will likely continue to drop in energy, leading to deformed ground states in lighter Z nuclei.

The location of the odd neutron can be determined from the single-particle level diagram shown in Fig. 3 and by reference to known states in the neutron-rich Fe isotopes. Contrary to simple expectations when bridging the  $N = 40$  gap, the ground states of  $^{65}\text{Fe}$  and  $^{67}\text{Fe}$  are tentatively assigned  $1/2^-$  spins and parities [27, 28]. The  $1/2^-$  ground-state spin and parity assignment of  $^{67}\text{Fe}$  was explained using a deformation of  $\sim 0.2$  [11]. Referring to Fig. 3, the most important neutron states at this deformation are a  $K = 1/2^-$  and  $K = 3/2^+$  originating from the spherical  $p_{1/2}$  and  $g_{9/2}$  single-particle states, respectively, for both  $N = 39$  and  $N = 41$  nuclei. The ground states in both  $^{65}\text{Fe}$  and  $^{67}\text{Fe}$  are attributed to filling the  $K = 1/2^-$  level, suggesting small changes occur to the energy separation between the  $\nu p_{1/2}$  and  $\nu f_{5/2}$  single-particle states between  $N = 39$  and  $N = 41$ . Further, based on half-life considerations for the unobserved isomeric level in  $^{67}\text{Fe}$ , an assignment of  $9/2^+$  [29] was excluded in favor of a  $5/2^+$  spin and parity due to the  $K = 5/2^+$  level of the neutron  $g_{9/2}$  single-particle state [11].

Based on the information from the Co and Fe isotopes, the ground states of  $^{64}\text{Mn}$  and  $^{66}\text{Mn}$  can be attributed to a proton in a  $K = 1/2^-$  state coupled with a neutron in a  $K = 1/2^-$  state, leading to a  $1^+$  ground-state spin and parity assignment. The first excited state in both nuclei is the result of coupling the odd proton to an odd neutron in the  $K = 3/2^+$  state originating from the neutron  $g_{9/2}$ , leading to a spin and parity of  $2^-$  (see Fig. 3). It is not possible to explain the low-energy isomeric  $4^+$  and  $5^-$  states in  $^{64}\text{Mn}$  and  $^{66}\text{Mn}$  using the available deformed neutron levels discussed previously and the  $K = 1/2^-$  proton level. The coupling of the proton  $K = 7/2^-$  level originating from the  $f_{7/2}$  single-particle state with either the neutron  $K = 1/2^-$  or  $K = 3/2^+$ , which could lead to the observed isomeric spins and parities, can be excluded based on the deformed coupling rules of Ref. [30].

However, if the coexistence of deformed and spherical states is considered the  $4^+$  and  $5^-$  isomeric states in  $^{64}\text{Mn}$  and  $^{66}\text{Mn}$  can be attributed to the spherical coupling between the  $\pi f_{7/2}$  and either the  $\pi p_{3/2}$  or  $\nu g_{9/2}$  single-particle states, respectively. The  $5^-$  level should be near the bottom of the multiplet formed from the coupling of the  $\pi f_{7/2}$  and  $\nu g_{9/2}$  orbits [31]. The hindrances of the  $M2$  isomers observed near  $N = 40$  for  $^{59m}\text{Cr}$ ,  $^{61m}\text{Fe}$ ,  $^{67m}\text{Ni}$ , and  $^{79m}\text{As}$  nuclei range between 12 and 24, significantly smaller than calculated for the  $M2$  isomer in  $^{66}\text{Mn}$ . The large hindrance of the  $^{66}\text{Mn}$  isomeric transition can be attributed to a shape transition between spherical and deformed configurations. The observed structural change from a spherical ground state in  $^{68}\text{Co}$  to a deformed ground state in  $^{66}\text{Mn}$  could be re-

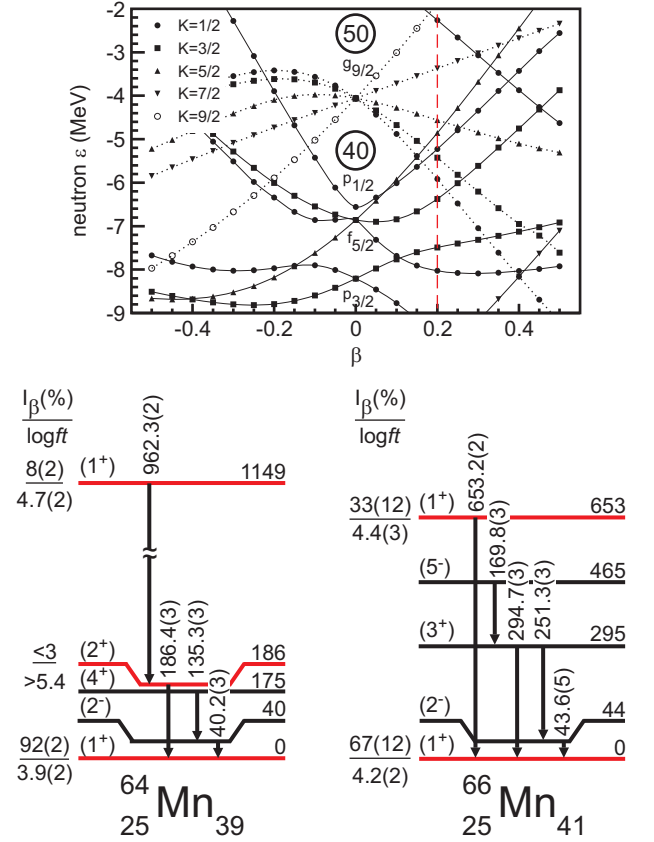


FIG. 3. (Color Online) (top) A Nilsson diagram encompassing the neutron  $p_{3/2}$ ,  $f_{5/2}$ ,  $p_{1/2}$ , and  $g_{9/2}$  single-particle states as a function of deformation. Dashed lines represent positive parity states. A red vertical dashed line at  $\beta = 0.2$  corresponds to the assumed deformation in the text. (bottom) Low-energy level structures deduced for  $^{64}\text{Mn}$  and  $^{66}\text{Mn}$  with tentatively assigned spins and parities. All indicated  $\gamma$ - $\gamma$  transitions were observed. The levels populated in  $\beta$  decay are displayed in red and the  $\beta$ -decay branching ratios and  $\log ft$  values are shown to the left of the state.  $\beta$ -decay  $Q$ -values were taken from Ref. [32]. States populated in the isomeric decays of  $^{64m}\text{Mn}$  and  $^{66m}\text{Mn}$  are indicated by black lines.

lated to the dramatic drop in various cross section measurements observed in Refs. [33, 34].

In conclusion, the low-energy level structures of  $^{64}\text{Mn}$  and  $^{66}\text{Mn}$  have been investigated through both the isomeric decay of metastable Mn states and the  $\beta$  decay of the respective  $^{64}\text{Cr}$  and  $^{66}\text{Cr}$  parent nuclei. Combined, both techniques give rise to a consistent picture in which spherical isomeric states coexist at low energy with deformed ground states in the Mn isotopes at a deformation around 0.2. Shape coexistence is proposed to be a key structural feature in this region and further experimental and theoretical work are required to explore the extent of this phenomenon in the  $N = 40$  region.

## ACKNOWLEDGMENTS

This work was funded in part by the NSF under contract NSF-0606007 and DOE under Contract

Nos. DE-AC02-06CH11357, DE-AC05-00OR22725, DE-FG02-94ER40834, DE-FG02-96ER40983, DE-FG02-96ER41006, and DOE Cooperative Agreement DE-FC03-03NA00143.

- 
- [1] M. Mayer and J. Jensen, in *Nobel Lectures in Physics 1963-1970* (Elsevier, Amsterdam, 1972)
- [2] T. Otsuka, T. Suzuki, M. Honma, Y. Utsuno, N. Tsunoda, K. Tsukiyama, and M. Hjorth-Jensen, *Phys. Rev. Lett.* **104**, 012501 (2010)
- [3] J. Dobaczewski, I. Hamamoto, W. Nazarewicz, and J. A. Sheikh, *Phys. Rev. Lett.* **72**, 981 (1994)
- [4] R. V. F. Janssens, *Nature*, 897 (2005)
- [5] J. L. Wood, K. Heyde, W. Nazarewicz, M. Huyse, and P. van Duppen, *Physics Reports* **215**, 101 (1992)
- [6] R. Broda, B. Fornal, W. Królas, T. Pawlat, D. Bazzacco, S. Lunardi, C. Rossi-Alvarez, R. Menegazzo, G. de Angelis, P. Bednarczyk, J. Rico, D. De Acuña, P. J. Daly, R. H. Mayer, M. Sferrazza, H. Grawe, K. H. Maier, and R. Schubart, *Phys. Rev. Lett.* **74**, 868 (1995)
- [7] M. Bernas, P. Dessagne, M. Langevin, J. Payet, F. Pougheon, and P. Roussel, *Physics Letters B* **113**, 279 (1982)
- [8] M. Hannawald, T. Kautzsch, A. Wöhr, W. B. Walters, K.-L. Kratz, V. N. Fedoseyev, V. I. Mishin, W. Böhmer, B. Pfeiffer, V. Sebastian, Y. Jading, U. Köster, J. Lettry, H. L. Ravn, and the ISOLDE Collaboration, *Phys. Rev. Lett.* **82**, 1391 (1999)
- [9] O. Sorlin, S. Leenhardt, C. Donzaud, J. Duprat, F. Azaiez, F. Nowacki, H. Grawe, Z. Dombrádi, F. Amorini, A. Astier, D. Baiborodin, M. Belleguic, C. Borcea, C. Bourgeois, D. M. Cullen, Z. Dlouhy, E. Dragulescu, M. Górski, S. Grévy, D. Guillemaud-Mueller, G. Hagemann, B. Herskind, J. Kiener, R. Lemmon, M. Lewitowicz, S. M. Lukyanov, P. Mayet, F. de Oliveira Santos, D. Pantalica, Y.-E. Penionzhkevich, F. Pougheon, A. Poves, N. Redon, M. G. Saint-Laurent, J. A. Scarpaci, G. Sletten, M. Stanoiu, O. Tarasov, and C. Theisen, *Phys. Rev. Lett.* **88**, 092501 (2002)
- [10] C. Guénaut, G. Audi, D. Beck, K. Blaum, G. Bollen, P. Delahaye, F. Herfurth, A. Kellerbauer, H.-J. Kluge, J. Libert, D. Lunney, S. Schwarz, L. Schweikhard, and C. Yazidjian, *Phys. Rev. C* **75**, 044303 (2007)
- [11] J.M.Daugas, I.Matea, J.-P.Delaroche, M.Pfutzner, M.Sawicka, F.Becker, G.Belier, C.R.Bingham, R.Borcea, E.Bouchez, A.Buta, E.Dragulescu, G.Georgiev, J.Giovinazzo, M.Girod, H.Grawe, R.Grzywacz, F.Hammache, F.Ibrahim, M.Lewitowicz, J.Libert, P.Mayet, V.Meot, F.Negoita, F. O. Santos, O.Perru, O.Roig, K.Rykaczewski, M.G.Saint-Laurent, J.E.Sauvestre, O.Sorlin, M.Stanoiu, I.Stefan, Ch.Stodel, Ch.Theisen, D.Verney, and J.Zylicz, *Phys. Rev. C* **83**, 054312 (2011), DOI:10.1103/PhysRevC.83.054312
- [12] W. Rother, A. Dewald, H. Iwasaki, S. M. Lenzi, K. Starosta, D. Bazin, T. Baugher, B. A. Brown, H. L. Crawford, C. Fransen, A. Gade, T. N. Ginter, T. Glasmacher, G. F. Grinyer, M. Hackstein, G. Ilie, J. Jolie, S. McDaniel, D. Miller, P. Petkov, T. Pissulla, A. Ratkiewicz, C. A. Ur, P. Voss, K. A. Walsh, D. Weishaar, and K.-O. Zell, *Phys. Rev. Lett.* **106**, 022502 (2011)
- [13] C. J. Chiara, I. Stefanescu, N. Hoteling, W. B. Walters, R. V. F. Janssens, R. Broda, M. P. Carpenter, B. Fornal, A. A. Hecht, W. Królas, T. Lauritsen, T. Pawlat, D. Seweryniak, X. Wang, A. Wöhr, J. Wrzesiński, and S. Zhu, *Phys. Rev. C* **82**, 054313 (2010)
- [14] J. J. Valiente-Dobón, S. M. Lenzi, S. J. Freeman, S. Lunardi, J. F. Smith, A. Gottardo, F. D. Vedova, E. Farnea, A. Gadea, D. R. Napoli, M. Axiotis, S. Aydin, D. Bazzacco, P. G. Bizzeti, A. M. Bizzeti-Sona, G. Benzoni, D. Bucurescu, L. Corradi, A. N. Deacon, G. De Angelis, E. Fioretto, B. Guiot, M. Ionescu-Bujor, A. Iordachescu, S. Leoni, N. Mărginean, R. Mărginean, P. Mason, R. Menegazzo, D. Mengoni, B. Million, G. Montagnoli, R. Orlandi, F. Recchia, E. Sahin, F. Scarlassara, R. P. Singh, A. M. Stefanini, D. Steppenbeck, S. Szilner, C. A. Ur, B. J. Varley, and O. Wieland, *Phys. Rev. C* **78**, 024302 (2008)
- [15] S. M. Lenzi, F. Nowacki, A. Poves, and K. Sieja, *Phys. Rev. C* **82**, 054301 (2010)
- [16] M. Sawicka, J. Daugas, H. Grawe, S. Cwiok, D. Balabanski, R. Braud, C. Bingham, C. Borcea, M. La Commar, G. de France, G. Georgiev, M. Grska, R. Grzywacz, M. Hass, M. Hellström, Z. Janas, M. Lewitowicz, H. Mach, I. Matea, G. Neyens, C. O' Leary, F. de Oliveira Santos, R. Page, M. Pfizner, Z. Podolyk, K. Rykaczewski, M. Stanoiu, and J. ylicz, *The European Physical Journal A - Hadrons and Nuclei* **16**, 51 (2003), 10.1140/epja/i2002-10073-1
- [17] D. Pauwels, O. Ivanov, N. Bree, J. Büscher, T. E. Cocolios, J. Gentens, M. Huyse, A. Korgul, Y. Kudryavtsev, R. Raabe, M. Sawicka, I. Stefanescu, J. Van de Walle, P. Van den Bergh, P. Van Duppen, and W. B. Walters, *Phys. Rev. C* **78**, 041307 (2008)
- [18] D. J. Morrissey, B. M. Sherrill, M. Steiner, A. Stolz, and I. Wiedenhoever, *Nucl. Instrum. Methods Phys. Res. B* **204**, 90 (2003)
- [19] J. I. Prisciandaro, A.C.Morton, and P. F.Mantica, *Nucl. Instrum. Methods Phys. Res. A* **505**, 140 (2003)
- [20] W. F. Mueller, J. A. Church, T. Glasmacher, D. Gutknecht, G. Hackman, P. G. Hansen, Z. Hu, K. L. Miller, and P. Quirin, *Nucl. Instrum. Methods Phys. Res. A* **466**, 492 (2001)
- [21] K. Starosta, C. Vaman, D. Miller, P. Voss, D. Bazin, T. Glasmacher, H. Crawford, P. Mantica, H. Tan, W. Hennig, M. Walby, A. Fallu-Labruyere, J. Harris, D. Breus, P. Grudberg, , and W. Warburton, *Nucl. Instrum. Methods Phys. Res. A* **610**, 700 (2009)
- [22] O. Sorlin, C. Donzaud, F. Azaiez, C. Bourgeois, L. Gaudefroy, F. Ibrahim, D. Guillemaud-Mueller, F. Pougheon, M. Lewitowicz, F. de Oliveira Santos, M. Saint-Laurent, M. Stanoiu, S. Lukyanov, Y. Penionzhkevich, J. Anglique, S. Grvy, K.-L. Kratz, B. Pfeiffer, F. Nowacki, Z. Dlouhy, and J. Mrasek, *Nuclear Physics A* **719**, C193 (2003)

- [23] L. Gaudefroy, O. Sorlin, C. Donzau, J. C. Angélique, F. Azaiez, C. Bourgeois, V. Chiste, Z. Dlouhy, S. Grévy, D. Guillemaud-Mueller, F. Ibrahim, K. L. Kratz, M. Lewitowicz, S. M. Lukyanov, I. Matea, J. Mrasek, F. Nowacki, F. de Oliveira Santos, Y. E. Penionzhkevich, B. Pfeiffer, F. Pougheon, M. G. Saint-Laurent, and M. Stanoiu, *The European Physical Journal A - Hadrons and Nuclei* **23**, 41 (2005), 10.1140/epja/i2004-10068-x
- [24] R. Grzywacz, R. Béraud, C. Borcea, A. Emsallem, M. Glógowski, H. Grawe, D. Guillemaud-Mueller, M. Hjorth-Jensen, M. Houry, M. Lewitowicz, A. C. Mueller, A. Nowak, A. Płochocki, M. Pfützner, K. Rykaczewski, M. G. Saint-Laurent, J. E. Sauvestre, M. Schaefer, O. Sorlin, J. Szerypo, W. Trinder, S. Viteritti, and J. Winfield, *Phys. Rev. Lett.* **81**, 766 (1998)
- [25] L. Gaudefroy, (2005)
- [26] P. Moller, J. R. Nix, and K. L. Kratz, *Atomic Data and Nuclear Data Tables* **66**, 131 (1997)
- [27] D. Pauwels, O. Ivanov, N. Bree, J. Büscher, T. E. Cocolios, M. Huyse, Y. Kudryavtsev, R. Raabe, M. Sawicka, J. V. de Walle, P. V. Duppen, A. Korgul, I. Stefanescu, A. A. Hecht, N. Hoteling, A. Wöhr, W. B. Walters, R. Broda, B. Fornal, W. Krolas, T. Pawlat, J. Wrzesinski, M. P. Carpenter, R. V. F. Janssens, T. Lauritsen, D. Seweryniak, S. Zhu, J. R. Stone, and X. Wang, *Phys. Rev. C* **79**, 044309 (2009)
- [28] J. M. Daugas, M. Sawicka, M. Pfützner, I. Matea, H. Grawe, R. Grzywacz, N. L. Achouri, J. C. Angélique, D. Baiborodin, F. Becker, G. Bélier, R. Bentida, R. Béraud, C. Bingham, C. Borcea, R. Borcea, E. Bouchez, A. Buta, W. N. Catford, E. Dragulescu, A. Emsallem, G. de France, J. Giovinozzo, M. Girod, H. Goutte, G. Gorgiev, K. L. Grzywacz-Jones, F. Hammache, F. Ibrahim, R. C. Lemmon, M. Lewitowicz, M. J. Lopez-Jimenez, P. Mayet, V. Méot, F. Negoita, F. de Oliveira-Santos, O. Perru, P. H. Regan, O. Roig, K. Rykaczewski, M. G. Saint-Laurent, J. E. Sauvestre, G. Sletten, O. Sorlin, M. Stanoiu, I. Stefan, C. Stodel, C. Theisen, D. Verney, and J. Zylicz, *AIP Conference Proceedings* **831**, 427 (2006)
- [29] M. Block, C. Bachelet, G. Bollen, M. Facina, C. M. Folden, C. Guenaut, A. A. Kwiatkowski, D. J. Morrissey, G. K. Pang, A. Prinke, R. Ringle, J. Savory, P. Schury, and S. Schwarz, *Phys. Rev. Lett.* **100**, 132501 (2008), DOI:10.1103/PhysRevLett.100.132501
- [30] C. J. Gallagher and S. A. Moszkowski, *Phys. Rev.* **111**, 1282 (1958)
- [31] V. Paar, *Nuclear Physics A* **331**, 16 (1979)
- [32] G. Audi, A. Wapstra, and C. Thibault, *Nuclear Physics A* **729**, 337 (2003), the 2003 NUBASE and Atomic Mass Evaluations
- [33] P. Adrich, A. M. Amthor, D. Bazin, M. D. Bowen, B. A. Brown, C. M. Campbell, J. M. Cook, A. Gade, D. Galaviz, T. Glasmacher, S. McDaniel, D. Miller, A. Obertelli, Y. Shimbara, K. P. Siwek, J. A. Tostevin, and D. Weisshaar, *Phys. Rev. C* **77**, 054306 (2008)
- [34] O. B. Tarasov, D. J. Morrissey, A. M. Amthor, T. Baumann, D. Bazin, A. Gade, T. N. Ginter, M. Hausmann, N. Inabe, T. Kubo, A. Nettleton, J. Pereira, M. Portillo, B. M. Sherrill, A. Stolz, and M. Thoennessen, *Phys. Rev. Lett.* **102**, 142501 (2009)